



Hydrothermal Carbonization of Sewage Sludge with Sawdust and Corn Stalk: Optimization of Process Parameters and Characterization of Hydrochar

Aria Shakiba¹ · Arash Aliasghar² · Khashayar Moazeni¹ · Maryam Pazoki¹

Received: 25 September 2022 / Accepted: 9 December 2022

© The Author(s), under exclusive licence to Springer Science+Business Media, LLC, part of Springer Nature 2023

Abstract

Disposal of sewage sludge (SS) is one of the problems in treatment plants; however, SS has a high-water volume and lacks some compounds and can be mixed with other biomass. The present study analyzed co-hydrothermal carbonization of sewage sludge with sawdust and corn stalk. This research aimed to optimize the process parameters, the temperature in the range of 180–300 °C, the reaction time in the range of 30–60 min, and pH in the range of 5–9 on the mass yield, energy yield, and high heat value (HHV) to increase the quality of hydrochar, and to analyze the effect of hydrothermal carbonization (HTC) on the characteristics of raw materials and hydrochar. The response surface method and Benken's box model were conducted using Design Expert 10 software. The optimal conditions for HHV, mass yield, and energy yield were 15.802 MJ/kg, 63.754%, and 67.415% respectively which occurred in the 205.358 °C, 30 min reaction time, and pH of 5. The temperature was the most influential parameter. The morphological, physicochemical, thermal, and crystalline properties of the hydrochar with the maximum HHV, mass yield and energy yield were evaluated as well. These results demonstrate that HTC is a suitable process to produce hydrochar, which can be used as a direct solid fuel.

Highlights

- Hydrothermal carbonization of sewage sludge with sawdust and cornstalk was investigated.
- Response surface optimization hydrothermal carbonization process was studied.
- The morphological, physicochemical, thermal, and crystalline properties of the hydrochar are reported.
- The optimal HHV was 15.802 MJ/kg.
- The process can produce hydrochar which can be used for direct combustion or activated carbon.

Keywords Hydrothermal carbonization · Biomass · Response surface methodology · Physicochemical characterization

Introduction

Today, factors such as the increase in the population of communities, the increase in water consumption, the production of sewage, and the increase in the amount of collected and treated sewage produce a large volume of sludge, making its proper management one of the challenges of the present century [1]. Sewage sludge (SS) is

a byproduct of urban sewage treatment processes, which can threaten human life due to the presence of pathogenic biological agents, viruses like SARS-CoV-2, and chemical compounds, including heavy metals. This is because, on the one hand, sludge disposal is associated with high costs, and on the other hand, environmental problems caused by sludge burial led to irreparable damage to the environment and humans [2]. The current epidemiological situation has prompted scientists to test sewage for the SARS-CoV-2 virus. Many studies confirm the presence of viruses in sewage that can be harmful for the environment [3, 4]. The most optimal alternative solutions for sludge stabilization are high temperature-based methods that eliminate pathogens [5]. The use of waste sludge as a renewable source for energy recovery is a suitable

✉ Arash Aliasghar
aaliasg1@stevens.edu

¹ Faculty of Environment, Tehran University, Tehran, Iran

² Department of Civil, Environmental & Ocean Engineering, Stevens Institute of Technology, Hoboken, NJ, USA

solution for how to manage the continuous increase in waste sludge production to strictly comply with environmental quality standards, as well as how to maintain a reliable and affordable energy supply for the current and future generations [6]. The use of sludge to produce renewable energy and heat has been the focus of various industries in recent years. The resulting benefits are manifested by a combination of factors such as reducing fossil fuel reserves due to increased demand for primary energy, increased fuel prices, climate change concerns, public awareness, and advances in renewable energy technologies [7]. Due to environmental, economic, social, and legal reasons, the treatment and disposal of excess sludge are among the serious crises in the biological treatment of sewage worldwide [8]. The two components in sludge that are technically and economically possible for recycling are nutrients (mainly nitrogen and phosphorus) and energy (carbon). However, because sewage sludge consists of approximately 98% water, in this research, sawdust (SD) and corn stalk waste (CS) are used as lignocellulosic biomass that have a high percentage of cellulose and lignin as feed together with sewage sludge, in order to achieve high-quality hydrochar [9]. Some of the existing or emerging energy recovery methods from SS are anaerobic digestion, incineration, and co-incineration of sludge in coal-fired power plants, conversion to gas, pyrolysis, and wet air oxidation, supercritical oxidation, and hydrothermal reaction, which is called hydrothermal carbonization (HTC) in the present study [10].

HTC is a method of thermal modification in a wet state, which converts organic compounds (e.g., biomass, SS, and organic wastes) in confined conditions into materials with different characteristics from the starting material. This process is performed in the temperature range of 150–350 °C, and the pressure conditions are self-contained (pressure caused by the activity of materials inside the reactor). One of the characteristics of HTC is the ability to process biomass in an aqueous environment. In general, SS contains excess water, while some types of biomass do not have water. However, co-hydrothermal carbonization of SS and sawdust and corn stalk can neutralize this factor to obtain favorable conditions [8]. This advanced process covers the HTC losses where a single feedstock is used. Many studies have shown that co-HTC increases the efficiency, HHV, thermal behavior, and overall quality of hydrochars compared to a single feedstock [11–13]. The HTC method has been recently used to change the structure of municipal solid waste, SS, and agricultural debris and turn it into more valuable and prosperous materials [14].

The conditions of the HTC process are fragile and variable, and many parameters affect the reactions that change the physical, chemical, and thermal characteristics of the produced hydrochar as an energy source [10]. HTC

is different from burning, gasification, and pyrolysis. It is conducted at a lower temperature and is more straightforward than the other methods. Furthermore, this method requires wet feed and is performed in the aqueous phase; thus, there is no need for initial drying. In HTC, the decomposition of raw materials, similar to the pyrolysis method, includes hydrolysis, dehydration, decarboxylation, aromatization, and recondensation [15]. Compared to other thermochemical methods, HTC has higher production efficiency than solid materials, and its aqueous phase has more soluble organic materials [16]. One of the advantages of HTC over the other methods is that wet heterogeneous organic materials and waste streams can react without separation and drying [17]. The produced hydrochar in the HTC method is more similar to natural coal than the produced char in pyrolysis. For this reason, more studies are being conducted on hydrochar applications. Despite the remarkable progress of these studies, this method is still unknown in many ways [15]. In the hydrolysis reaction, as one of the main and often the most fundamental reactions in the conversion of organic substances, the primary molecule depends on parameters affecting the hydrothermal process, including the effect of temperature, the impact of residence time, the result of the type of feed, and the outcome of the catalyst [18]. The hydrochar can be used as an absorbent and catalyst based on the aromatic structure and functional groups on its surface. Some gas, oil, and the main product of the hydrochar are produced if the HTC process is performed on biomass. Hydrochar can be employed as a soil conditioner, absorbent, activated carbon, and fuel [17, 19].

In the sludge treatment process, dewatering plays an important role in minimizing sludge volume, increasing heating value, facilitating transportation, and even reducing leachate production in landfills. HTC can be an effective method to increase the dewatering properties of sludge [20].

The HTC product is a mixture that can be separated into solid and liquid parts. Its liquid fraction (LFHTC) contains at least 15% of primary carbon and can be used as a potential source of chemicals or fuel. Also, it can be used as a feedstock in aerobic digestion, anaerobic digestion, and wet air oxidation [21].

In a comparative study by Wilk et al. [13] on the HTC of two types of lignocellulosic biomass (pine and acacia) and SS, raw materials were all placed under the same conditions for 4 h at a temperature of 200 °C and a ratio of water to materials of 1:8. Lignocellulosic biomass had increased energy-related properties, while the effect of HTC on SS was negligible due to the more incredible conversion of carbon into the liquid phase [13]. In the study on the HTC of SS, a type of microalgae, and a combination of them, Lee et al. [23] found that the production efficiency of solid construction in SS increased with the addition of this

microalgae. This combination has increased the HHV and the quality of the produced coal (the H/C and O/C ratio). In addition, M. Puccini et al. [24] optimized the conversion of hydrochar from SS to HTC using the response surface method. The parameters of temperature, time, and the ratio of solid input material were considered in the optimization. The physical, chemical, and morphological characteristics of the produced hydrochar were investigated, showing that the water absorption capacity, HHV, and carbon content increased in the hydrochar compared to raw materials [24].

This work was conducted to investigate the effect of different parameters on the HTC process of SS with corn stalks and sawdust. A novel aspect of this study is its attempt to find optimal processes which use RSM and to consider energy yield, mass yield, and HHV as responses. This paper also examined char properties more comprehensively. Thermogravimetric analysis (TGA), Fourier-transform infrared (FT-IR) spectroscopy, X-ray diffraction (XRD), and scanning electron microscopy (SEM) are also employed to analyze the change in characteristics during the HTC process.

Materials and Methods

In this study, the lignocellulosic biomass of corn stalks and sawdust were used, along with secondary or activated SS collected from the wastewater treatment plant in Ekbatan Town, Iran. Sample preparation included drying, crushing, and sieving. For drying, SS was kept at 105 °C for 24 h, and sawdust and corn stalks were maintained at 40 °C for 24 h in an oven (Shimadzu Co.). SS was crushed by a planetary ball mill, and sawdust and corn stalks were crushed by a home mill. SS was sieved through a No. 60 mesh (0.25 mm), which passes particles smaller than 0.25 mm, and sawdust and corn stalks were sieved through a sieve with a No. 18 mesh (1 mm), which passes particles smaller than 1 mm [8].

After the preparation steps mentioned earlier, sewage sludge, sawdust, and corn stalks were mixed in 20 cc of deionized water in the ratio 1:1:1:12 by a magnet and stirrer for 15 min. The reason for using deionized water is that it is free from any ions, which makes the process accurate. All the measurements were performed in triplicate.

The applied reactor in this study was a tubular type (Batch Reactor) with a body of 316 stainless steel and a volume of 75 mL. A device (Model FlashEA 1112, Thermo Finnigan Company) was used to measure the carbon, oxygen, nitrogen, sulfur, and hydrogen percentages of hydrochar samples. Finally, 20 mg of each sample was placed in the machine in a powdered form. Furthermore, a thermal weighing analyzer (TGA, TA Company, USA) was employed to continuously measure the weight loss

due to the decomposition or loss of water. Moreover, a Fourier-transform infrared (FT-IR) spectrophotometer (Thermo Fisher Company, USA) was utilized to check the structure of the prepared hydrochar samples. A scanning electron microscope (SEM, model MIRA III, TESCAN, Czech Republic) was used for the samples' surface morphology and particle size by checking the electron microscope technique. Likewise, the PW1730 device (PHILIPS) was applied for X-ray diffraction (XRD, model PW1730, PHILIPS) analysis. Step size and time per step were used as a routine laboratory (0.05 degrees and 1 s, respectively), and the goniometer angle was chosen from 10 to 80 degrees.

The three independent study parameters of temperature in the range of 180–300 °C, reaction time in the range of 30–60 min, and pH in the range of 5–9 were selected to analyze their effect on the process. 0.1 M HCl acid and 0.1 M NaOH base were used to adjust the pH of the samples.

The studied answer in this research is the HHV, the most essential factor for investigating hydrochar as a fuel. The experiment design was performed to examine the effect of crucial parameters on the efficiency of HTC using the Box-Benken method by Design Expert software, version 10. Finally, the maximum HHV, mass yield, and energy yield sample (The bolded numbers in the Table 1) were investigated to measure TGA, FT-IR, SEM, and XRD.

Results and Discussion

Elemental Analysis Test Results

The feedstock and the hydrochars have been investigated in the laboratory of Tehran University, and the results, including the percentage of each element of carbon, hydrogen, nitrogen, sulfur, and oxygen, have been obtained. According to the percentage of elements according to the Dulong relationship, the high heat value of each sample has been obtained, which is shown in Table 1, along with mass yield and energy yield.

The Results of the Experiment Design Software

Based on our findings in Table 1, the highest HHV was obtained at the temperature of 300 °C and the reaction time of 45 min. In addition, the highest mass yield and energy yield occurred at the temperature of 180 °C and the reaction time of 30 min. Accordingly, the temperature was more influential compared to the reaction time, which was not far from expectation due to the thermochemical nature of the hydrothermal process [25]. The results revealed that the produced hydrochar after the conversion had more

Table 1 Experimental design

Test order	Parameters			Response		
	Reaction time (A)	Temperature (B)	pH (C)	High heat value (MJ/kg)	Mass yield (%)	Energy yield (%)
1	60	180	7	13.61	45.7	49.75
2	60	240	5	15.05	37.3	44.91
3	60	300	7	15.9	30.2	38.4
4	45	240	7	15.88	40.4	51.33
5	30	300	7	16.11	34.4	44.32
6	60	240	9	16.36	39.3	51.43
7	45	300	5	16.79	33.1	44.46
8	30	180	7	14.96	56.5	67.61
9	30	240	5	16.51	46.8	61.79
10	45	180	5	14.12	52	58.75
11	45	240	7	15.83	41	51.92
12	45	180	9	15.26	50.6	61.78
13	45	300	9	16.28	31.7	41.27
14	30	240	9	16.35	43.1	56.38
15	45	240	7	15.9	40.6	51.65

carbon and hydrogen and less oxygen compared to raw materials [26]. The increasing HHV and the amount of carbon in the samples demonstrate that the chemical bonds of oxygen have been destroyed during the hydrothermal process [18].

HHV

According to the results of the experiments, the software has proposed a quadratic model for the HHV. Furthermore, the formula fitted to the results using the quadratic model is in the form of the following relationship.

$$\text{HHV} = 15.78 - 0.38 (A) + 0.89 (B) + 0.22 (C) + 0.28 (A)(B) + 0.36 (A)(C) - 0.41 (B)(C) - 0.14 (A^2) - 0.59 (B^2) + 0.33 (C^2)$$

A: Reaction time, B: Temperature, C: pH

Table 2 provides the analysis of variance (ANOVA) of the obtained results from experiments related to the HHV. The *p* value is less than 0.0001, which is less than 0.05, representing the high significance of the quadratic model. Therefore, the probability of a coefficient other than the one presented in the equation is less than 5%. Hence, the given model (level two) is significant. Furthermore, the lack of fit test is meaningless with a value of 0.086, indicating a significant relationship between the parameters as influential factors and the HHV as the response.

Table 3 presents the value of R^2 or compatibility of the experimental data with the obtained data, implying that 99% of our information equals the predicted data, but R^2 alone is not enough, and terms that have no effect are ignored in adjusted R^2 , and forecasts have played a role as well. Predicted R^2 represents how powerful our model is for

prediction. According to the software, the difference between adjusted and predicted R^2 should be less than 0.2, which is acceptable in this model. C.V.% is the change coefficient; the lower it is, the better it will be, showing that the data changes are less [19, 27].

Effect of Reaction Time and Temperature on the HHV

Fig. 1A displays the three-dimensional diagram of the simultaneous effect of temperature and reaction time on the HHV of the produced hydrochar by the HTC method. In this situation, other parameters affecting the HHV are considered constant in their central values. As shown, the amount of the HHV has changed the most with an increase in temperature, and as expected, the temperature was the most influential parameter because there is a more remarkable change in the graph of the HHV compared to temperature [22]. The dielectric constant of water dramatically decreases with increasing temperature, and in subcritical conditions, the value of the dielectric constant (ϵ) of water decreases from 80 to 20. By reducing the dielectric constant, the properties of water have become highly similar to organic solvents [28]. As a result, water can dissolve other organic compounds and become a single liquid phase. The advantages of being single-phase are the greater concentration of the reactant, leading to the occurrence of more reactions, while the inter-phase mass transfer does not occur and does not cause a problem in the speed of the process [29]. In the subcritical region, water's ionic constant (K_w) increases up to three times the water environment. The low dielectric constant allows subcritical water to dissolve organic compounds; on the other hand, the high ionization constant creates an acidic environment to perform the hydrolysis

Table 2 Results of the analysis of variance of the HHV

Source	Sum of squares	df	Mean square	F value	p value prob > F	
Model	11.29	9	1.25	133.97	<0.0001	Significant
A-time	1.13	1	1.13	121.05	0.0001	
B-temperature	6.34	1	6.34	677.12	<0.0001	
C-pH	0.40	1	0.40	42.25	0.0013	
AB	0.32	1	0.32	34.61	0.0020	
AC	0.53	1	0.53	56.88	0.0006	
BC	0.68	1	0.68	73.09	0.0004	
A ²	0.070	1	0.070	7.51	0.0408	
B ²	1.29	1	1.29	138.16	<0.0001	
C ²	0.41	1	0.41	43.75	0.0012	
Residual	0.047	5	9.360E-003			
Lack of fit	0.044	3	0.015	10.68	0.0868	Not significant
Pure error	2.749E-003	2	1.374E-003			
Cor total	11.33	14				

Table 3 General statistical data

SD	0.097	R ²	0.9959
Mean	15.66	Adjusted R ²	0.9884
C.V. %	0.62	Predicted R ²	0.9373

SD, standard deviation; C.V., coefficient of variation

reaction as well as possible [22]. Based on the obtained data, the HHV decreases with an increase in the retention time, indicating that the reactions progress in the direction that the produced liquid fuel increases and the HHV of the hydrochar decreases; another reason is the presence of sludge in the raw material, which contains a little carbohydrate and is mainly composed of fat and proteins [30, 31].

Fig. 1 **a** Three-dimensional diagram of the effect of temperature and reaction time on the HHV. **b** Three-dimensional diagram of the effect of temperature and pH on the HHV. **c** Three-dimensional diagram of the effect of reaction time and pH on the HHV.

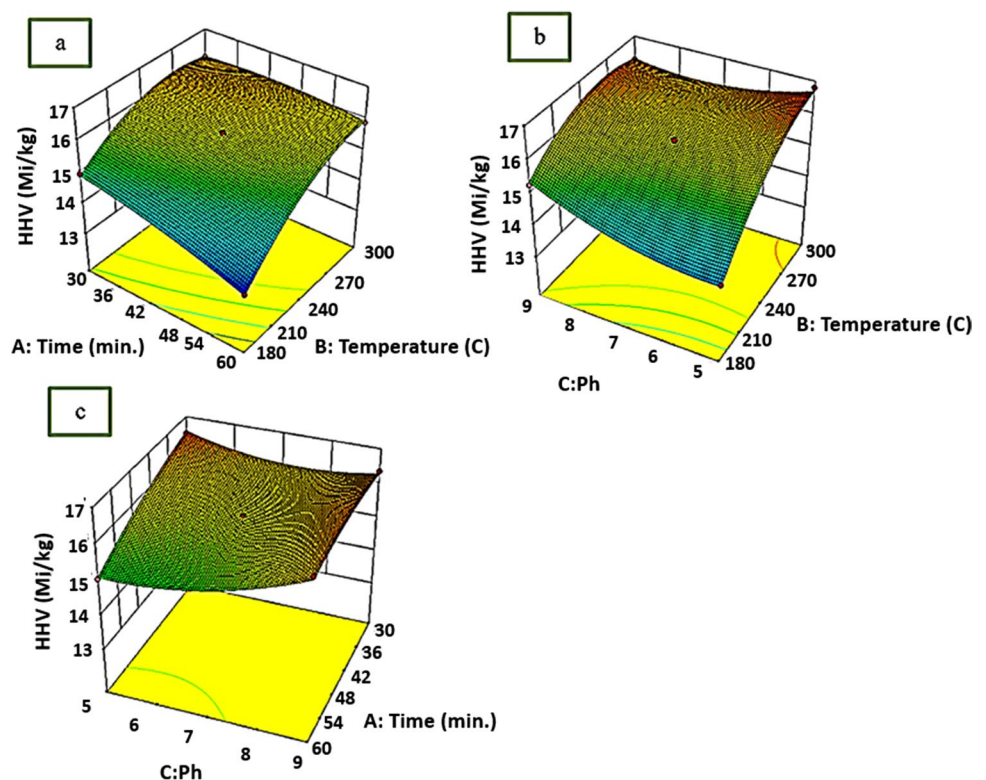
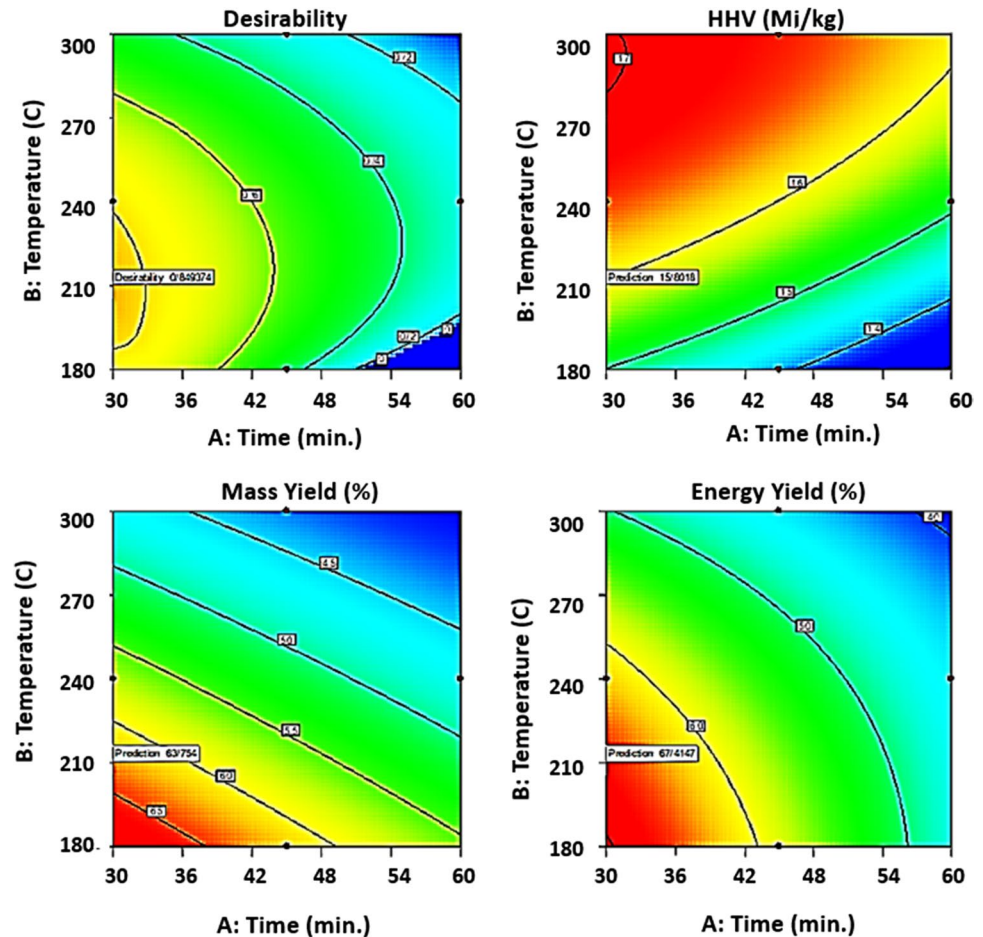


Fig. 2 The graph of optimal conditions



Effect of Temperature and pH on the HHV

The three-dimensional diagram of the simultaneous effect of temperature and pH on the HHV of the produced hydrochar by the HTC method is illustrated in Fig. 1b. In this case, other factors affecting the HHV are considered fixed in their central values. Furthermore, pH was in the range of 5–9 and did not cause much change in the HHV. In fact, the temperature has caused more noticeable changes than pH. However, even in these small changes, the HHV is higher in an acidic state. One of the reasons for the higher HHV is that the hydrolysis process happens faster in acidic environments. Furthermore, the dehydration reaction of organic materials increased [29]. The pH does not have that much effect on the HHV in this range because there are many changes in the pH of water as a buffer in the hydrothermal process and the reactions direct the pH [32].

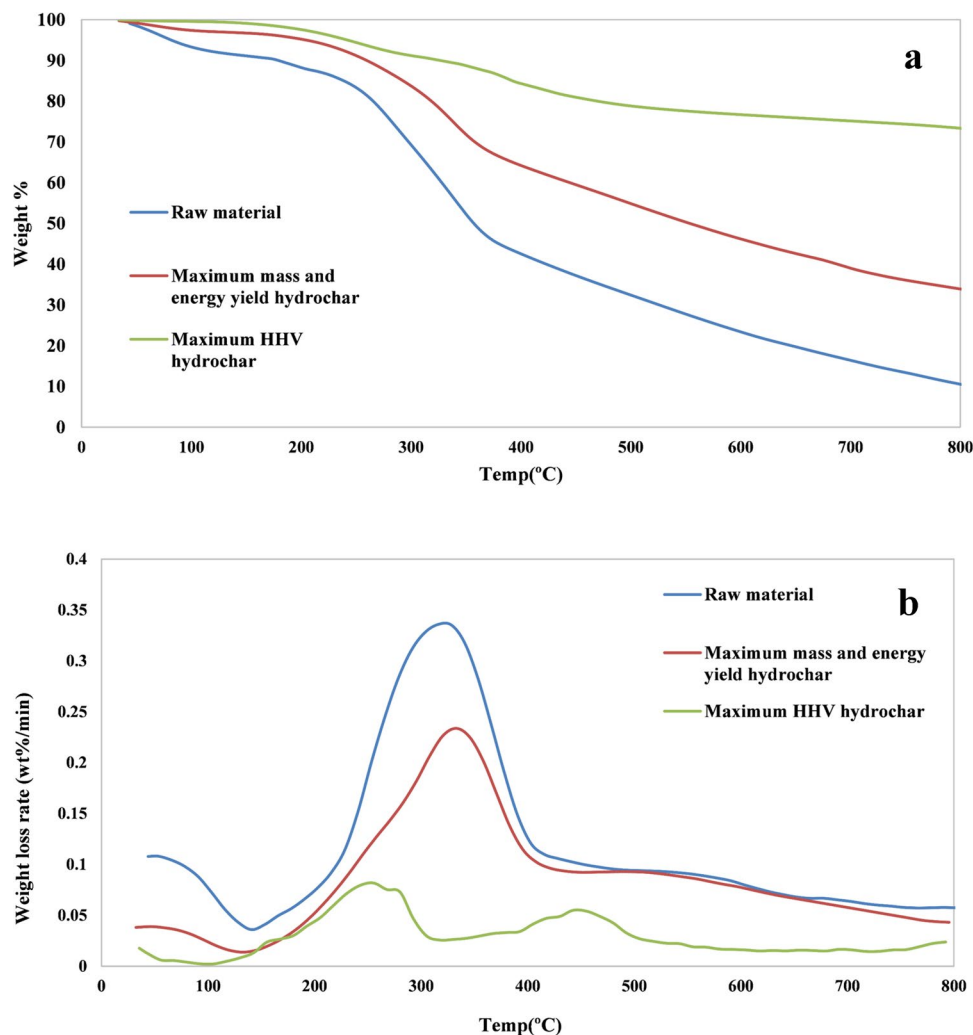
Effect of Reaction Time and pH on the HHV

Fig. 1c displays the three-dimensional diagram of the simultaneous effect of the reaction time and pH on the HHV of the hydrochar produced by the HTC method. In this case, other factors influencing the HHV are considered constant in their central values. As shown, the reaction time and pH do not cause many changes in the HHV, and the range of their differences is not extremely large. However, in the same low amount, the HHV is higher in less time and has lower pH. Low pH and higher HHV promote hydrolysis and dehydration processes. Moreover, the pH decreases at the beginning of the hydrothermal method, and if the environment is acidic, it causes the reaction to occur as quickly as possible [33].

Test Optimization

According to the Design Expert 10 software, the optimal HHV, mass yield, and energy yield occur at a temperature of

Fig. 3 **a** TGA diagrams of samples. **b** DTG diagram of samples. *Note.* TGA, thermal weighing analyzer; DTG, derivative thermogravimetric curve.



205.358 °C, a reaction time of 30 min, and a pH of 5, which is equivalent to 15.802 MJ/Kg, 63.754%, and 67.415%, respectively.

The utility provided by the software for compatibility of the equations with the input data and the generated graphs was 0.849, which is considered a significant value for utility. Among the eight solutions and answers that the software has obtained to solve its mathematical equations, solution number 1 is the most desirable among 41 solutions, the results of which are illustrated in Fig. 2. Due to the insignificant effect of pH on the resulting responses, the optimization graphs based on temperature and time are provided here.

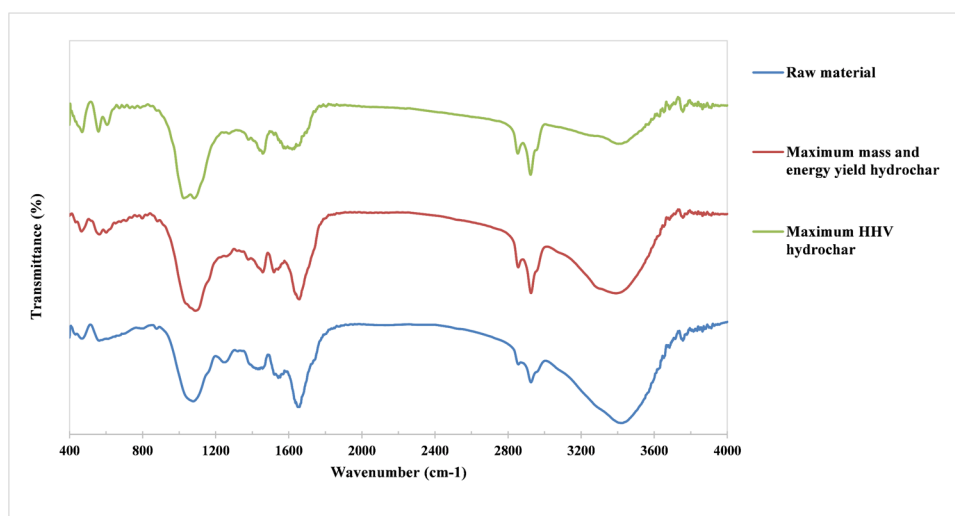
Investigation of the Characteristics of Production Hydrochars and Raw Materials

Maximum HHV hydrochar, maximum mass yield and energy yield of hydrochar and raw material were evaluated for their physicochemical properties, morphology, and thermal decomposition. Also, TGA, FT-IR, SEM, and XRD tests were performed on them accordingly.

TGA Results

A TGA test and its derivative thermogravimetric (DTG) curve have been conducted to study the thermal decomposition behavior of raw materials and hydrochar. As depicted in Fig. 3 a and b, thermal decomposition has three main stages. The first stage (25–200 °C) is slow weight loss due to the removal of moisture and some volatile substances [34]. The combustion of raw materials mainly includes the combustion of volatile materials and moisture, which occurs at low temperatures. The second stage (200–400 °C) is the decomposition of the most volatile substances, as well as cellulose and hemicellulose [33]. A gradual weight loss is observed at temperatures above 400 °C and up to 500 °C, which is attributed to the slow thermal decomposition of lignin. At higher temperatures and up to 800 °C, the last stage of decomposition, the weight loss is as raw materials > maximum mass and energy yield > maximum HHV, which is inversely proportional to the carbon content of the samples; in other

Fig. 4 Graph of FT-IR results.
Note. FT-IR, Fourier-transform infrared spectroscopy



words, the sample with a higher HHV has more fixed carbon and shows that the temperature stability of hydrochar has improved compared to raw materials [35]. The horizontal lines in the TGA charts indicate the stability range and temperature range in which there is no change in the mass of the sample by an increase in the temperature [36]. According to the DTG diagrams, the concentrated decomposition in the raw material at the peak of $C^{\circ}321$ starts earlier than the hydrochar. The maximum weight loss of the hydrochar (the maximum HHV) is transferred to higher temperatures, indicating cellulose decomposition.

FT-IR Results

Figure 4 illustrates the FT-IR diagram of raw materials and hydrochar. The main factor groups in the sample seem almost the same. The ranges of raw materials and hydrochar are similar, showing that the HTC process had a slight effect on the functional groups, and HTC was stable [37]. Considering that the raw material contains cellulose, a functional group can be observed at 3200–13,600 cm. The peak at 13,400 cm is related to the active hydroxyl group (-OH). Two peaks in the range of 13,000–2800 cm^{-1} in the sample are alkane and aldehyde functional groups in cellulose. The peak in the 1600–11,800-cm range belongs to the carbonyl (C=O) and carboxyl (C=C) bond, which becomes weaker after HTC. The peaks between 1400 and 11,600 cm are associated with the bonding of alkanes (-CH₂) in the aromatic ring. The peaks in the range of 1000–11,200 cm are related to ether and ester bonds, which are intensified in hydrochar and indicate the dehydration of alcohol [38, 39].

SEM Results

The morphological properties of raw materials and hydrochar by SEM are depicted in Fig. 5. The structural integrity of hydrochar was reduced and fragmented compared to raw materials. The hydrochar surfaces were rougher and harder than raw materials, and porous surfaces were observed on the hydrochar surface. This feature is because the samples were at different degrees of decomposition during HTC, which destroyed biopolymers such as cellulose, hemicellulose, and lignin, and more porous surfaces. The hydrochar of the maximum HHV (b) contains a smaller number of fibrous structures, which indicates the complete decomposition of raw materials during the formation of the hydrochar. The HTC process increases the porosity of raw materials, which can increase access to air and its distribution, leading to a higher combustion reaction [40]. M. Puccini et al. [24] also found that porosity increases in hydrochar samples due to dehydration and the release of volatile substances [24]. In addition, porous properties can be used for other applications, including removing pollutants (as adsorbents). In the study of L. Wang et al., raw materials only included corn stalks, and the central point biochar was rougher and more fragile [41], but these changes are less in the hydrochar of our research.

XRD Results

The XRD diagram of raw materials and hydrochar is displayed in Fig. 6. As shown, the intensity of the peaks in hydrochar has increased compared to that in raw materials, implying that the HTC process has increased the crystalline properties of raw materials. The increase in crystalline

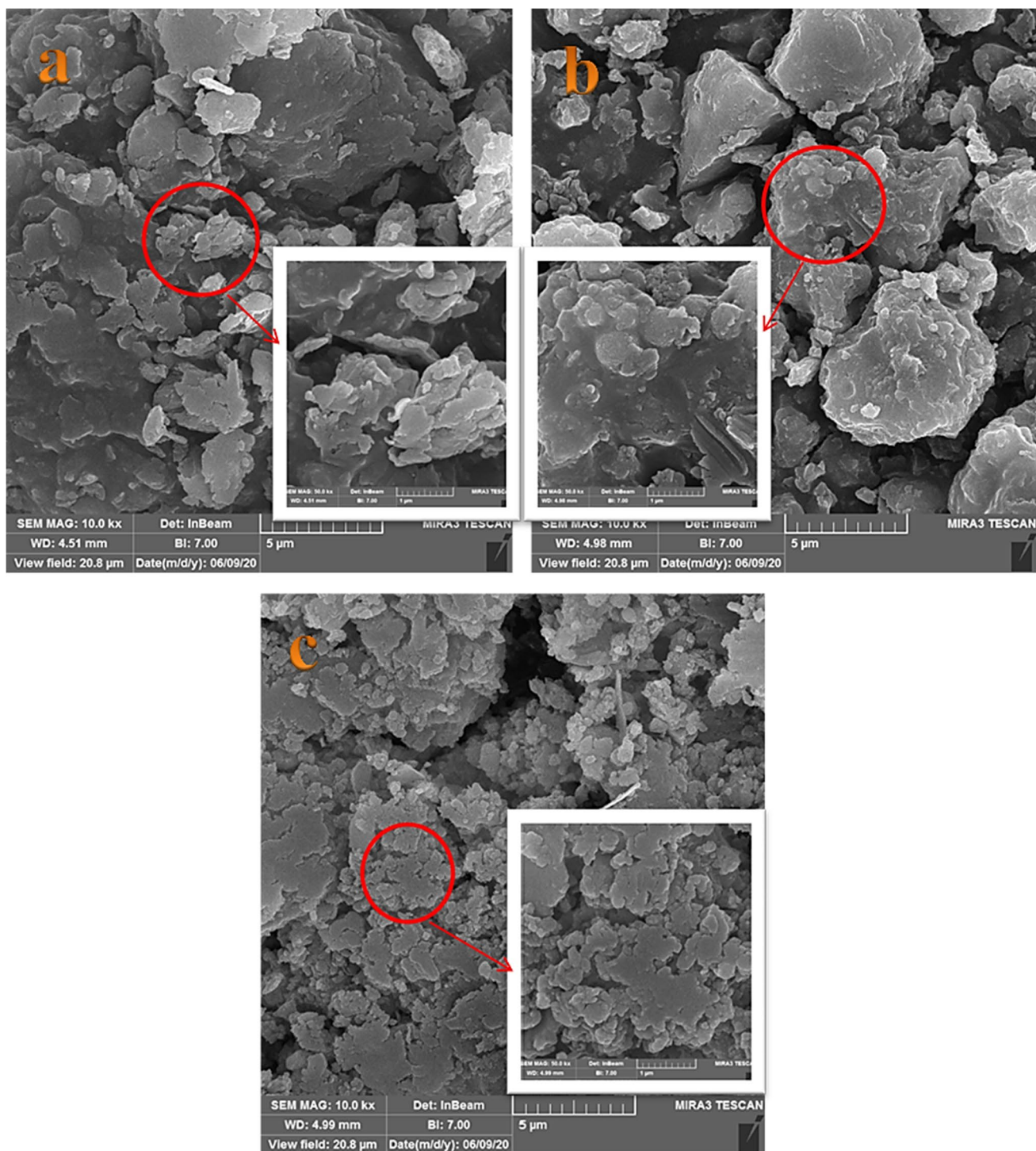
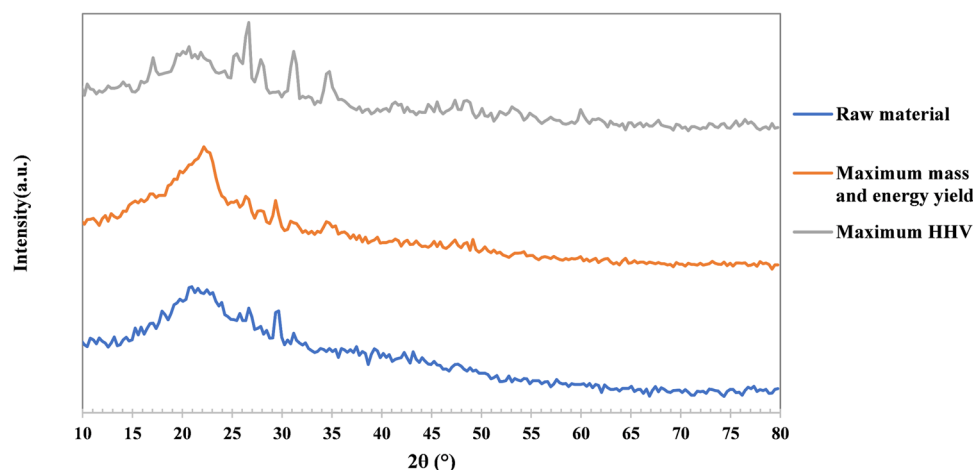


Fig. 5 SEM images: **a** raw materials, **b** maximum HHV hydrochar, and **c** maximum mass and energy yield of hydrochar. *Note.* SEM, scanning electron microscopy

properties can be related to the removal of amorphous compounds (compounds that do not have crystalline order) such as lignin and hemicellulose [42]. The data were analyzed and reported using Xpert software. Two peaks at 17°

and 22° represent the crystalline coordinates of cellulose, and the peak at 34.7° is associated with hemicellulose [43]. The peaks observed at 17° and 22° of hydrochar are more intense than of the raw materials, indicating that they

Fig. 6 Graph of XRD results.
Note. XRD, X-ray diffraction



are aromatic. These intensities show that aromatization has increased during the increase of compounds such as graphite [44]. It also confirms the destruction of cellulose in the hydrothermal carbonization process.

Conclusion

By the HTC process, the carbon percentage increased, and their oxygen percentage decreased. The results of the Design Expert software revealed that temperature had the most significant effect on the HHV. The increase in temperature was associated with the decrease of oxygenated functional groups. The TGA test indicated that the thermal stability increased after HTC, and hydrochar was destroyed at higher temperatures than raw materials, and it can be used for direct combustion or combustion with a percentage of coal. The SEM and XRD tests revealed that the hydrochar was separated, fragmented, and crystallized, and the surface porosity represented an increase. The spherical molecules were removed from the surface of the hydrochar by the decomposition of cellulose and hemicellulose; the changes were more noticeable in the hydrochar. Compared to raw materials, maximum HHV hydrochar revealed properties similar to high-quality coal with the addition of sawdust and corn stalk to SS.

Acknowledgements We graciously acknowledge the support of Tehran University for the use of their facilities.

Author Contribution Aria Shakiba: conceptualization, writing – original draft, visualization, methodology, investigation, formal analysis. Arash Aliasghar: conceptualization, writing – original draft, methodology, investigation, formal analysis. Khashayar Moazeni: writing – review and editing. Maryam Pazoki: supervision, project administration.

Data Availability The datasets used and/or analyzed during the current study are available from the corresponding author on reasonable request.

References

1. Quan LM, Kamyab H, Yuzir A, Ashokkumar V, Hosseini SE, Balasubramanian B, Kirpichnikova I (2022) Review of the application of gasification and combustion technology and waste-to-energy technologies in sewage sludge treatment. *Fuel* 316:123199. <https://doi.org/10.1016/J.FUEL.2022.123199>
2. Hatinoğlu MD, Sanin FD (2021) Sewage sludge as a source of microplastics in the environment: a review of occurrence and fate during sludge treatment. *J Environ Manage* 295:113028. <https://doi.org/10.1016/J.JENVMAN.2021.113028>
3. Westhaus S, Weber FA, Schiwy S, Linnemann V, Brinkmann M, Widera M, Greve C, Janke A, Hollert H, Wintgens T, Ciesek S (2021) Detection of SARS-CoV-2 in raw and treated wastewater in Germany – suitability for COVID-19 surveillance and potential transmission risks. *Sci Total Environ* 751:141750. <https://doi.org/10.1016/J.SCITOTENV.2020.141750>
4. Randazzo W, Truchado P, Cuevas-Ferrando E, Simón P, Allende A, Sánchez G (2020) SARS-CoV-2 RNA in wastewater anticipated COVID-19 occurrence in a low prevalence area. *Water Res* 181:115942. <https://doi.org/10.1016/J.WATRES.2020.115942>
5. Carraturo F, Del Giudice C, Morelli M, Cerullo V, Libralato G, Galdiero E, Guida M (2020) Persistence of SARS-CoV-2 in the environment and COVID-19 transmission risk from environmental matrices and surfaces. *Environ Pollut* 265:115010. <https://doi.org/10.1016/J.ENVPOL.2020.115010>
6. Zhai Y, Peng C, Xu B, Wang T, Li C, Zeng G, Zhu Y (2017) Hydrothermal carbonisation of sewage sludge for char production with different waste biomass: effects of reaction temperature and energy recycling. *Energy* 127:167–174
7. Mateo-Sagasta J, Raschid-Sally L, Thebo A (2015) Global wastewater and sludge production, treatment and use. In *Wastewater*. Springer, Dordrecht, pp. 15–38
8. Kambo HS, Dutta A (2015) A comparative review of biochar and hydrochar in terms of production, physico-chemical properties

- and applications. *Renew Sustain Energy Rev* 45:359–378. <https://doi.org/10.1016/j.rser.2015.01.050>
9. Wilk M, Śliz M, Lubieniecki B (2021) Hydrothermal co-carbonization of sewage sludge and fuel additives: combustion performance of hydrochar. *Renewable Energy* 178:1046–1056. <https://doi.org/10.1016/J.RENENE.2021.06.101>
 10. Xi Lu, Berge ND (2014) Influence of feedstock chemical composition on product formation and characteristics derived from the hydrothermal carbonization of mixed feedstocks. *Biores Technol* 166:120–131
 11. Xi Lu, Ma XX, Chen X (2021) Co-hydrothermal carbonization of sewage sludge and lignocellulosic biomass: fuel properties and heavy metal transformation behaviour of hydrochars. *Energy* 221:119896. <https://doi.org/10.1016/J.ENERGY.2021.119896>
 12. Wang R, Lin K, Ren D, Peng P, Zhao Z, Yin Q, Gao P (2022) Energy conversion performance in co-hydrothermal carbonization of sewage sludge and pinewood sawdust coupling with anaerobic digestion of the produced wastewater. *Sci Total Environ* 803:149964. <https://doi.org/10.1016/J.SCITOTENV.2021.149964>
 13. Wilk M, Magdziarz A, Jayaraman K, Szymańska-Chargot M, Gökalp I (2019) Hydrothermal carbonization characteristics of sewage sludge and lignocellulosic biomass. A comparative study. *Biomass Bioenergy* 120:166–175
 14. Lu Xi, Pellechia PJ, Flora JRV, Berge ND (2013) Influence of reaction time and temperature on product formation and characteristics associated with the hydrothermal carbonization of cellulose. *Biores Technol* 138:180–190
 15. Paraknowitsch JP, Thomas A, Antonietti M (2009) Carbon colloids prepared by hydrothermal carbonization as efficient fuel for indirect carbon fuel cells. *Chem Mater* 21(7):1170–1172
 16. Nizamuddin S, Baloch HA, Griffin GJ, Mubarak NM, Bhutto AW, Abro R, Mazari SA, Ali BS (2017) An overview of effect of process parameters on hydrothermal carbonization of biomass. *Renew Sustain Energy Rev* 73:1289–1299
 17. Fang J, Zhan L, Ok YS, Gao B (2018) Minireview of potential applications of hydrochar derived from hydrothermal carbonization of biomass. *J Ind Eng Chem* 57:15–21
 18. Sevilla M, Fuertes AB (2009) The production of carbon materials by hydrothermal carbonization of cellulose. *Carbon* 47(9):2281–2289. <https://doi.org/10.1016/J.CARBON.2009.04.026>
 19. Ferreira SLC, Bruns RE, Ferreira HS, Matos GD, David JM, Brandão GC, da Silva EGP, Portugal LA, dos Reis PS, Souza S, dos Santos WNL (2007) Box-Behnken design: an alternative for the optimization of analytical methods. *Anal Chim Acta* 597(2):179–186. <https://doi.org/10.1016/J.ACA.2007.07.011>
 20. Wu B, Dai X, Chai X (2020) Critical review on dewatering of sewage sludge: influential mechanism, conditioning technologies and implications to sludge re-utilizations. *Water Res* 180:115912. <https://doi.org/10.1016/J.WATRES.2020.115912>
 21. Malhotra M, Garg A (2020) Hydrothermal carbonization of centrifuged sewage sludge: determination of resource recovery from liquid fraction and thermal behaviour of hydrochar. *Waste Manage* 117:114–123. <https://doi.org/10.1016/J.WASMAN.2020.07.026>
 22. Peterson A, Vogel F, Lachance R et al (2022) Thermochemical biofuel production in hydrothermal media: a review of sub- and supercritical water technologies. *Energy Environ Sci* 1(1):32–65
 23. Lee J, Sohn D, Lee K, Park KY (2019) Solid fuel production through hydrothermal carbonization of sewage sludge and microalgae *Chlorella* sp. from wastewater treatment plant. *Chemosphere* 230:157–163. <https://doi.org/10.1016/J.CHEMOSPHERE.2019.05.066>
 24. Puccini M, Tasca A L, Gemma M, Raspolli A, Vitolo S, Riccardo G (2019) Hydrothermal carbonization of sewage sludge: process optimization by response surface methodology
 25. González-Arias J, Sánchez ME, Cara-Jiménez J, Baena-Moreno FM, Zhang Z (2022) Hydrothermal carbonization of biomass and waste: a review. *Environ Chem Lett* 20(1):211–221. <https://doi.org/10.1007/S10311-021-01311-X/TABLES/2>
 26. Wang Q, Wu S, Cui D, Zhou H, Wu D, Pan S, Xu F, Wang Z (2022) Co-hydrothermal carbonization of organic solid wastes to hydrochar as potential fuel: a review. *Sci Total Environ* 850:158034. <https://doi.org/10.1016/J.SCITOTENV.2022.158034>
 27. Akbari H, Akbari H, Fanaei F, Adibzadeh A (2022) Optimization of parameters affecting the hydrothermal carbonization of wastewater treatment plant sewage sludge. *Biomass Convers Biorefinery* 1–12. <https://doi.org/10.1007/S13399-022-03427-8/FIGURES/6>
 28. Titirici M, Thomas A, Antonietti M (2007) Back in the black: hydrothermal carbonization of plant material as an efficient chemical process to treat the CO₂ problem?. *New J Chem* 31(6):787–789
 29. Sun X, Sumida H, Yoshikawa K (2013) Effects of hydrothermal process on the nutrient release of sewage sludge. *Int J Waste Resour.* 3(2):0–0. <https://doi.org/10.4172/2252-5211.1000124>
 30. Yin F, Chen H, Xu G, Wang G, Xu Y (2015) A detailed kinetic model for the hydrothermal decomposition process of sewage sludge. *Bioresour Technol* 198:351–357. <https://doi.org/10.1016/J.BIORTECH.2015.09.033>
 31. Cao Y, He M, Dutta S, Luo G, Zhang S, Tsang D (2021) Hydrothermal carbonization and liquefaction for sustainable production of hydrochar and aromatics. *Renew Sustain Energy Rev* 152:111722. <https://doi.org/10.1016/J.RSER.2021.111722>
 32. Liu X, Fan Y, Zhai Y, Liu X, Wang Z, Zhu Y, Shi H, Li C, Zhu Y (2022) Co-hydrothermal carbonization of rape straw and microalgae: pH-enhanced carbonization process to obtain clean hydrochar. *Energy* 257:124733. <https://doi.org/10.1016/J.ENERGY.2022.124733>
 33. He C, Wang K, Yang Y, Wang JY (2014) Utilization of sewage-sludge-derived hydrochars toward efficient cocombustion with different-rank coals: effects of subcritical water conversion and blending scenarios. *Energy Fuels* 28(9):6140–6150. https://doi.org/10.1021/EF501386G/ASSET/IMAGES/LARGE/EF-2014-01386G_0005.JPEG
 34. Magdziarz A, Werle S (2014) Analysis of the combustion and pyrolysis of dried sewage sludge by TGA and MS. *Waste Manage* 34(1):174–179. <https://doi.org/10.1016/J.WASMAN.2013.10.033>
 35. Xi Lu, Ma XX, Qin Z, Ke C, Chen L, Chen X (2021) Co-hydrothermal carbonization of sewage sludge with wood chip: fuel properties and heavy metal transformation behavior of hydrochars. *Energy and Fuels* 35(19):15790–15801. https://doi.org/10.1021/ACS.ENERGYFUELS.1C02145/SUPPL_FILE/EFIC02145_SI_001.PDF
 36. Jayaraman K, Kok MV, Gokalp I (2016) Combustion properties and kinetics of different biomass samples using TG–MS technique. *J Therm Anal Calorim* 127(2):1361–1370. <https://doi.org/10.1007/S10973-016-6042-1>
 37. Areeprasert C, Zhao P, Ma D, Shen Y, Yoshikawa K (2014) Alternative solid fuel production from paper sludge employing hydrothermal treatment. *Energy Fuels* 28(2):1198–1206. https://doi.org/10.1021/EF402371H/ASSET/IMAGES/LARGE/EF-2013-02371H_0010.JPEG
 38. Peng C, Zhai Y, Zhu Y, Xu B, Wang T, Li C, Zeng G (2016) Production of char from sewage sludge employing hydrothermal carbonization: char properties, combustion behavior and thermal

- characteristics. *Fuel* 176:110–118. <https://doi.org/10.1016/J.FUEL.2016.02.068>
39. Xi Lu, Ma X, Qin Z, Chen X, Yue W (2022) Co-hydrothermal carbonization of sewage sludge and swine manure: hydrochar properties and heavy metal chemical speciation. *Fuel* 330:125573. <https://doi.org/10.1016/J.FUEL.2022.125573>
40. Gaur RZ, Khoury O, Zohar M, Poverenov E, Darzi R, Laor Y, Posmanik R (2020) Hydrothermal carbonization of sewage sludge coupled with anaerobic digestion: integrated approach for sludge management and energy recycling. *Energy Convers Manage* 224:113353. <https://doi.org/10.1016/j.enconman.2020.113353>
41. Wang L, Chang Y, Li A (2019) Hydrothermal carbonization for energy-efficient processing of sewage sludge: a review. *Renew Sustain Energy Rev* 108:423–440. <https://doi.org/10.1016/J.RSER.2019.04.011>
42. Nanda S, Mohanty P, Pant KK, Naik S, Kozinski JA, Dalai AK (2013) Characterization of North American lignocellulosic biomass and biochars in terms of their candidacy for alternate renewable fuels. *Bioenergy Res* 6(2):663–677. <https://doi.org/10.1007/S12155-012-9281-4/TABLES/5>
43. Guo S, Dong X, Wu T, Shi F, Zhu C (2015) Characteristic evolution of hydrochar from hydrothermal carbonization of corn stalk. *J Anal Appl Pyrol* 116:1–9. <https://doi.org/10.1016/J.JAAP.2015.10.015>
44. Azargohar R, Nanda S, Kozinski JA, Dalai AK, Sutarto R (2014) Effects of temperature on the physicochemical characteristics of fast pyrolysis bio-chars derived from Canadian waste biomass. *Fuel* 125:90–100. <https://doi.org/10.1016/J.FUEL.2014.01.083>

Publisher's Note Springer Nature remains neutral with regard to jurisdictional claims in published maps and institutional affiliations.

Springer Nature or its licensor (e.g. a society or other partner) holds exclusive rights to this article under a publishing agreement with the author(s) or other rightsholder(s); author self-archiving of the accepted manuscript version of this article is solely governed by the terms of such publishing agreement and applicable law.